World Journal of Gastroenterology

Submit a Manuscript: https://www.f6publishing.com

World J Gastroenterol 2018 December 28; 24(48): 5477-5490

DOI: 10.3748/wjg.v24.i48.5477

ISSN 1007-9327 (print) ISSN 2219-2840 (online)

ORIGINAL ARTICLE

Basic Study

Mismatched effects of receptor interacting protein kinase-3 on hepatic steatosis and inflammation in non-alcoholic fatty liver disease

Waqar Khalid Saeed, Dae Won Jun, Kiseok Jang, Sang Bong Ahn, Ju Hee Oh, Yeon Ji Chae, Jai Sun Lee, Hyeon Tae Kang

Waqar Khalid Saeed, Dae Won Jun, Department of Gastroenterology, Hanyang University College of Medicine, Seoul 04763, South Korea

Kiseok Jang, Department of Pathology, Hanyang University College of Medicine, Seoul 04763, South Korea

Sang Bong Ahn, Department of Internal Medicine, Eulji University, Daejeon 34824, South Korea

Ju Hee Oh, Yeon Ji Chae, Jai Sun Lee, Hyeon Tae Kang, Department of Translational Medicine, Hanyang University College of Medicine, Seoul 04763, South Korea

ORCID number: Waqar Khalid Saeed (0000-0002-7888-9108); Dae Won Jun (0000-0002-2875-6139); Kiseok Jang (0000-0002-6585-3990); Sang Bong Ahn (0000-0001-7419-5259); Ju Hee Oh (0000-0003-3031-0272); Yeon Ji Chae (0000-0001-7126-1070); Jai Sun Lee (0000-0002-1673-8777); Hyeon Tae Kang (0000-0002-0595-3025).

Author contributions: Saeed WK drafted the manuscript; Jun DW designed the research and supervised the project; Oh JH, Chae YJ, Lee JS, and Kang HT collected the data; Lee JS analyzed the data; Jang K analyzed the histology data; Ahn SB supervised and revised the manuscript.

Supported by National Research Foundation of Korea (NRF), funded by the South Korean Government, No. NRF-2017M3A9C8028794.

Institutional animal care and use committee statement: All the experimental procedures were approved by the Hanyang University Institutional Animal Care and Use Committee of (HY-IACUC-16-0075).

Conflict-of-interest statement: The authors have declared no conflicts of interest.

Data sharing statement: No additional data is available.

Manuscript source: Unsolicited manuscript

Corresponding author: Dae Won Jun, MD, PhD, Professor, Department of Internal Medicine, Hanyang University College of Medicine, 222-1 Wangsimni-ro, Seongdong-gu, Seoul 04763, South Korea. noshin@hanyang.ac.kr
Telephone: +82-2-22908338
Fax: +82-2-9720068

Received: August 27, 2018
Peer-review started: August 27, 2018
First decision: October 24, 2018
Revised: November 8, 2018
Accepted: November 13, 2018
Article in press: November 13, 2018
Published online: December 28, 2018

Abstract

AIM

To validate the effects of receptor interacting protein kinase-3 (RIP3) deletion in non-alcoholic fatty liver disease (NAFLD) and to clarify the mechanism of action.

METHODS

Wild-type (WT) and RIP3 knockout (KO) mice were

fed normal chow and high fat (HF) diets for 12 wk. The body weight was assessed once weekly. After 12 wk, the liver and serum samples were extracted. The liver tissue expression levels of RIP3, microsomal triglyceride transfer protein, protein disulfide isomerase, apolipoprotein-B, X-box binding protein-1, sterol regulatory element-binding protein-1c, fatty acid synthase, cluster of differentiation-36, diglyceride acyltransferase, peroxisome proliferator-activated receptor alpha, tumor necrosis factor-alpha (TNF-α), and interleukin-6 were assessed. Oleic acid treated primary hepatocytes from WT and RIP3KO mice were stained with Nile red. The expression of inflammatory cytokines, including chemokine (C-X-C motif) ligand (CXCL) 1, CXCL2, and TNF-α, in monocytes was evaluated.

RESULTS

RIP3KO HF diet fed mice showed a significant gain in body weight, and liver weight, liver to body weight ratio, and liver triglycerides were increased in HF diet fed RIP3KO mice compared to HF diet fed WT mice. RIP3KO primary hepatocytes also had increased intracellular fat droplets compared to WT primary hepatocytes after oleic acid treatment. RIP3 overexpression decreased hepatic fat content. Quantitative real-time polymerase chain reaction analysis showed that the expression of very-low-density lipoproteins secretion markers (microsomal triglyceride transfer protein, protein disulfide isomerase, and apolipoprotein-B) was significantly suppressed in RIP3KO mice. The overall NAFLD Activity Score was the same between WT and RIP3KO mice; however, RIP3KO mice had increased fatty change and decreased lobular inflammation compared to WT mice. Inflammatory signals (CXCL1/2, TNF-α, and interleukin-6) increased after lipopolysaccharide and pan-caspase inhibitor (necroptotic condition) treatment in monocytes. Neutrophil chemokines (CXCL1, and CXCL2) were decreased, and TNF-α was increased after RIP3 inhibitor treatment in monocytes.

CONCLUSION

RIP3 deletion exacerbates steatosis, and partially inhibits inflammation in the HF diet induced NAFLD model.

Key words: Necroptosis; Receptor interacting protein kinase-3; Mixed lineage kinase domain-like protein; Non-alcoholic fatty liver disease; Steatosis

Core tip: Receptor interacting protein kinase-3 (RIP3) deletion was associated with increased fatty change, hepatic tissue triglycerides, body weight, and serum aspartate aminotransferase and alanine aminotransferase levels. Very-low-density lipoproteins secretion markers, including apolipoprotein-B, microsomal triglyceride transfer protein, and protein disulfide isomerase, were suppressed with RIP3 deletion. High fat diet fed RIP3KO mice had reduced expressions of tumor necrosis factor alpha and neutrophil chemokines [Chemokine (C-X-C motif) ligands: CXCL1, and CXCL2] compared to high fat diet fed wild-type mice. *In vitro* analysis suggests that necroptotic stimulation [lipopolysaccharide + N-Benzyloxycarbonyl-Val-Ala-Asp(O-Me) fluoromethyl ketone] increased CXCL1/2 expression in monocytes. Treatment with RIP3 inhibitor (GSK'843) decreased the expression of CXCL1/2 as well as interleukin-6.

Saeed WK, Jun DW, Jang K, Ahn SB, Oh JH, Chae YJ, Lee JS, Kang HT. Mismatched effects of receptor interacting protein kinase-3 on hepatic steatosis and inflammation in non-alcoholic fatty liver disease. *World J Gastroenterol* 2018; 24(48): 5477-5490
URL: https://www.wjgnet.com/1007-9327/full/v24/i48/5477.htm
DOI: https://dx.doi.org/10.3748/wjg.v24.i48.5477

INTRODUCTION

Non-alcoholic fatty liver disease (NAFLD) comprises one of the major liver disease burden in the developed world. In the United States, the prevalence of NAFLD is up to 25%[1]. NAFLD, the hepatic component of metabolic syndrome, is a multifactorial wide spectrum disease ranging from simple steatosis to steatohepatitis and further progressing to fibrosis and hepatocellular carcinoma. In NAFLD, increased lipid accumulation in hepatocytes leads to steatosis, inflammation, and fibrosis. NAFLD could also be hinting towards decreasing heart function[2]. In younger patients, NAFLD is also associated with decreased sleep, decreased quality and frequency of food intake, and a sedentary life-style[3]. The lifestyle modifications directed towards reduced steatosis in NAFLD would not only improve NAFLD but also cardiac function[2]. Although the prevalence of NAFLD is increasing, there are still numerous diagnostic and treatment issues associated with NAFLD. For instance, liver biopsy remains the gold standard method for NAFLD diagnosis, but currently no diagnostic method can correctly distinguish between simple steatosis and steatohepatitis. Moreover, there is still a lack of a satisfactory treatment strategy for NAFLD[4].

In NAFLD, the 'first hit' comprises of accumulation of fatty acids in hepatocytes facilitated by increased fatty acid synthesis and increased insulin resistance. Later, the multiple 'parallel hits' mainly comprising of endoplasmic reticulum stress, mitochondrial dysfunction, oxidative stress, and inflammatory cytokines further facilitate hepatocyte dysfunction and death[5]. Cell death is the fundamental step leading to steatohepatitis from benign steatosis. The increased steatosis and inflammation can trigger hepatocyte death by either apoptosis or necrosis[6-8]. Recently, the significance of inhibiting alternate cell death pathways including necroptosis has been extensively reported[9].

Necroptosis, which is a receptor interacting protein kinase 1 and 3 (RIP1/RIP3) and mixed lineage kinase domain like pseudokinase (MLKL) dependent, apoptosis alternative, and necrosis like cell death pathway, has been evaluated in various hepatic pathologies[10-17]. The increased expression of RIP3 and MLKL observed in human NASH, type II diabetes, and obese patients[11-13] highlights the significance of necroptosis in human metabolic disease conditions. Moreover, human metabolic disease serum markers, including HbA1c and insulin, are also correlated with RIP3 and *p*-MLKL expression[13].

Previously, several studies reported varying results on necroptosis inhibition in animal NAFLD models[11-13,18]. To evaluate the role of necroptosis inhibition, the studies utilized methionine choline deficient (MCD) diet, high fat (HF) diet, and choline-deficient HF diet (CD-HFD) induced-NAFLD models[11-13,18]. In the HF diet-induced NAFLD model, RIP3 inhibition led to increased steatosis and glucose intolerance[13,18]. The global RIP3 deletion led to increased body weight and hepatic steatosis in the HF diet-induced NAFLD model, while in the MCD diet-induced NAFLD model, RIP3 deletion showed protective effects on both hepatic steatosis and inflammation[11,12]. Interestingly, HF diet fed RIP3KO mice also had increased hepatic apoptosis, inflammation, and fibrosis[18]. Moreover, adipose tissue apoptosis and inflammation were also increased in RIP3KO mice compared to WT mice[13,18]. An additional *in vivo* signaling pathway was suspected which led to increased steatosis[13,18], adipocyte apoptosis, and inflammation[13]. On contrary, in the MCD diet-induced NAFLD model, RIP3KO mice had decreased inflammation, steatosis, and fibrosis compared to WT mice[11,12]. Although the previous studies evaluated the effect of RIP3 deletion in the HF diet-induced NAFLD model, the detailed mechanism of increased steatosis associated with RIP3 deletion was not clear.

Therefore, by using HF diet-induced NAFLD in RIP3KO mice, we aimed to validate and evaluate the precise underlying mechanism of steatosis and inflammation in hepatocytes and inflammatory cells.

MATERIALS AND METHODS

Animal experiments

C57BL/6 wild-type (WT) (8-9 wk old) and RIP3-KO mice (8-9 wk old) were randomly divided into following groups (n = 8); WT- normal chow (NC), WT-HF, RIP3KO-NC, and RIP3KO-HF. To evaluate the effects of RIP3 inhibition on HF diet-induced NAFLD development, NC and HF (60% kcal) diets were fed for 12 wk to the assigned groups. Four animals were kept per cage and animals were maintained in a temperature-controlled room (22 ℃) on a 12:12 h light-dark cycle. The body weight was recorded once weekly. After 12 wk, the animals were sacrificed. The liver weight and liver to body weight ratio were measured. All the experimental procedures were approved by the Hanyang University Institutional Animal Care and Use Committee of (HY-IACUC-16-0075). RIP3-KO animals were generously provided by Newton *et al*[19] Genentech (San Francisco, CA, United States).

Histological assessment of liver biopsy samples

For histological assessment, paraformaldehyde fixed, paraffin embedded liver tissue samples were sectioned (4 μm) and stained with hematoxylin & eosin. The stained liver biopsy samples were analyzed by a single pathologist. The NASH clinical research network scoring system was used to histologically grade the NAFLD in mice liver[20]. Briefly, steatosis degree, hepatocyte ballooning, and lobular inflammation were graded semi-quantitatively. The NAFLD Activity Score (NAS) was assessed by a combination of each score. Based on the NAS score, the commutative score of (0-2), control; (3-4), NAFLD; and (> 5), NASH was assigned.

Triglyceride quantification

To quantify liver triglycerides (TG) content, a TG quantification kit (Abcam, Cambridge, MA, United States) was used. Briefly, snap-frozen livers tissues (50–100 mg) were homogenized in 5% NP-40, and then slowly heated to 80 ℃ for 5 min and cooled down. The process was repeated twice. The samples were then centrifuged for 5 min, and supernatants were diluted 20-fold with distilled water and analyzed calorimetrically according to manufacturer's instructions.

HepG2 cells culture and maintenance

HepG2 cells were seeded on 6-well plate using Dulbecco's modified Eagle's medium (DMEM; Gibco, Grand Island, NY, United States) containing 10% fetal bovine serum (FBS) and 1% penicillin/streptomycin (P/S). After 24 h, the media was removed, and the cells were washed with Dulbecco's phosphate-buffered saline (DPBS) followed by treatment with oleic acid (OA; 400 μmol/L; Sigma-Aldrich, St Louis, MO, United States), palmitic acid (PA; 400 μmol/L; Sigma-Aldrich), and GSK' 843 (5 μmol/L; AOBIOUS INC, Gloucester, MA, United States). After 24 h, the RNA was isolated using the RNeasy mini kit (Qiagen, Hilden, Germany) according to manufacturer's instructions.

Primary hepatocytes isolation and culture

Primary hepatocytes from WT and RIP3-KO mice were isolated by a two-step collagenase perfusion method as described previously[21]. Briefly, mice were anesthetized using Zoletil and Rompun 1:1. The liver was perfused using calcium and magnesium-free Hanks' Balanced Salt Solution (HBSS; Welgene, Gyeongsan, South Korea) supplemented with 25 mmol/L, 4-(2-hydroxyethyl)-1-piperazine ethanesulfonic acid (HEPES; Amresco, Solon, OH, United States) and 0.5 mmol/L, ethylene-

glycol-bis-(β-aminoethylene)-N,N,N′,N′-tetraacetic acid (EGTA; Sigma-Aldrich), followed by perfusion with low glucose DMEM supplemented with 15 mmol/L HEPES and Collagenase Type IV (100 U/mL; Worthington Biochemical Corporation, Lakewood, NJ, United States) (pH 7.4, 37 ℃). After perfusion, the liver was carefully removed and gently minced in 20 mL ice-cold William' s E medium (Gibco) supplemented with 10% heat-inactivated FBS, 10 mL/L insulin-transferrin-selenium (ITS; Gibco), and 10 mL/L P/S. The homogenized liver suspension was filtered using a 70 μm cell strainer. The cell suspension was centrifuged at 50 × *g* for 5 min. The pellet was re-suspended in 10 mL William's Medium supplemented with 10% FBS, ITS (10 mL/L), P/S (10 mL/L), and 10 mL buffered Percoll (Sigma-Aldrich). The resultant cell suspension was centrifuged at 50 × *g* for 5 min, and the pellet re-suspended in William's E medium supplemented with 10% FBS, ITS (10 mL/L), and 1 μmol/L dexamethasone and P/S (10 mL/L). The cell viability was determined using the Trypan Blue exclusion method and was generally > 85%. After isolation, primary hepatocytes were plated on rat-tail collagen I (Corning Inc., Corning, NY, United States) coated culture dishes (Thermo Fisher Scientific Inc., Waltham, MA, United States) at 3 × 10^5 cells/mL. The hepatocytes were maintained at 37 ℃ in a humidified atmosphere of 5% CO_2 for 4 h. After 4 h, the media were removed, and cells were treated with OA (400 μmol/L) in serum-free William's E medium containing ITS (10 mL/L), 1 μmol/L dexamethasone, and P/S (10 mL/L). The control group was treated with equal volumes of dimethyl sulfoxide (DMSO). After 24 h, the hepatocytes were processed as per experimental protocols.

Macrophage cell culture and maintenance

The macrophage U937 cell line was used. The cells were seeded on 6-well plates using DMEM supplemented with 10% FBS and 1% P/S. After 24 h, the media were removed, and the cells were washed with DPBS followed by incubation with tumor necrosis factor alpha (TNF-α) (10 ng/mL; R&D Systems, Minneapolis, MN, United States), N-benzyloxycarbonyl-Val-Ala-Asp(O-Me) fluoromethyl ketone (zVAD) (30 μmol/L, R&D Systems), lipopolysaccharide (LPS) (25 ng/mL; Sigma-Aldrich), and GSK'843 (5 μmol/L). After 24 h, the RNA was isolated using the RNeasy mini kit (Qiagen) according to manufactures instructions.

Serum biochemical analysis

The whole blood samples collected in Becton Dickinson serum separation tubes (Franklin Lakes, NJ, United States) were centrifuged at 3000 rpm at 4 ℃ for 10 min. The serum samples were collected and stored at -80 ℃ until analysis. Serum alanine aminotransferase (ALT), aspartate aminotransferase (AST), and TG were measured with an automatic chemical analyzer (Hitachi-747; Hitachi, Tokyo, Japan).

Nile red staining

For lipid droplet staining, primary hepatocytes and HepG2 cells were seeded on a coverslip and maintained for 4 and 24 h, respectively. After adherence, the media were removed and cells were co-treated with OA (400 μmol/L) and GSK'843 (5 μmol/L). The control groups were treated with equal volumes of DMSO. After 24 h, the media were removed, and the cells were washed twice with DPBS, fixed with 4% paraformaldehyde in PBS for 30 min at room temperature, rinsed twice with DPBS, and incubated with fluorescence dye Nile red (0.5 mg/mL in acetone). The confocal imaging was performed using a Leica TCS SP5 confocal microscope (Leica Microsystems, Wetzlar, Germany).

RIP3 non-viral vector construction

The human RIP3 (NM_006871) coding regions were amplified by polymerase chain reaction (PCR) using TrueORF cDNA Clones (Origene, Rockville, MD, United States) for genes. The fragments were cloned into the pECFP (enhanced green fluorescent protein)-C1 vector (Clontech, Palo Alto, CA, United States). Later, RIP3 PCR products were subcloned into the pGEM-T easy vector (Promega, Madison, WI, United States) and then cloned into the EcoRI - BamHI sites of the pECFP-C1 vector.

RIP3 overexpression in primary hepatocytes

The primary hepatocytes were isolated and maintained as previously described. RIP3 was overexpressed in primary hepatocytes using JetPEI DNA transfection reagent (Polyplus-transfection SA, Illkirch, France) according to the manufacturer's instructions. Briefly, 1 × 10^5/mL primary hepatocytes were seeded on collagen-coated cover slides in 24-well plates. After 4 h, the media were replaced with fresh culture media supplemented with 10% FBS. RIP3 DNA (3 μg/well) was diluted in 100 μL NaCl (150 mmol/L) and was gently vortexed and spun down. Six microliters per well JetPEI reagent was diluted in 100 μL NaCl (150 mmol/L) and was gently vortexed and spun down. The diluted reagent was mixed and vortexed with diluted DNA and incubated for 30 min at room temperature. After 30 min, 50 μL JetPEI/DNA mix was added to each well of a 24-well plate. After 12 h, the transfection was confirmed by visualizing green fluorescence of EGFP-C1 using a Leica DMI 14000B inverted microscope (Leica Microsystems).

RNA isolation and quantitative real-time PCR

Total liver RNA was isolated from liver tissue using the TRIzol Reagent (Invitrogen, Carlsbad, CA, United States) according to the manufacturer's instructions. The isolated RNA samples were converted to cDNA using reverse transcriptase (SuperScript III; Invitrogen) and oligo (dT) primers. All PCR reactions were performed on the LightCycler 480 system (Roche Diagnostics, Mannheim, Germany) using LightCycler480

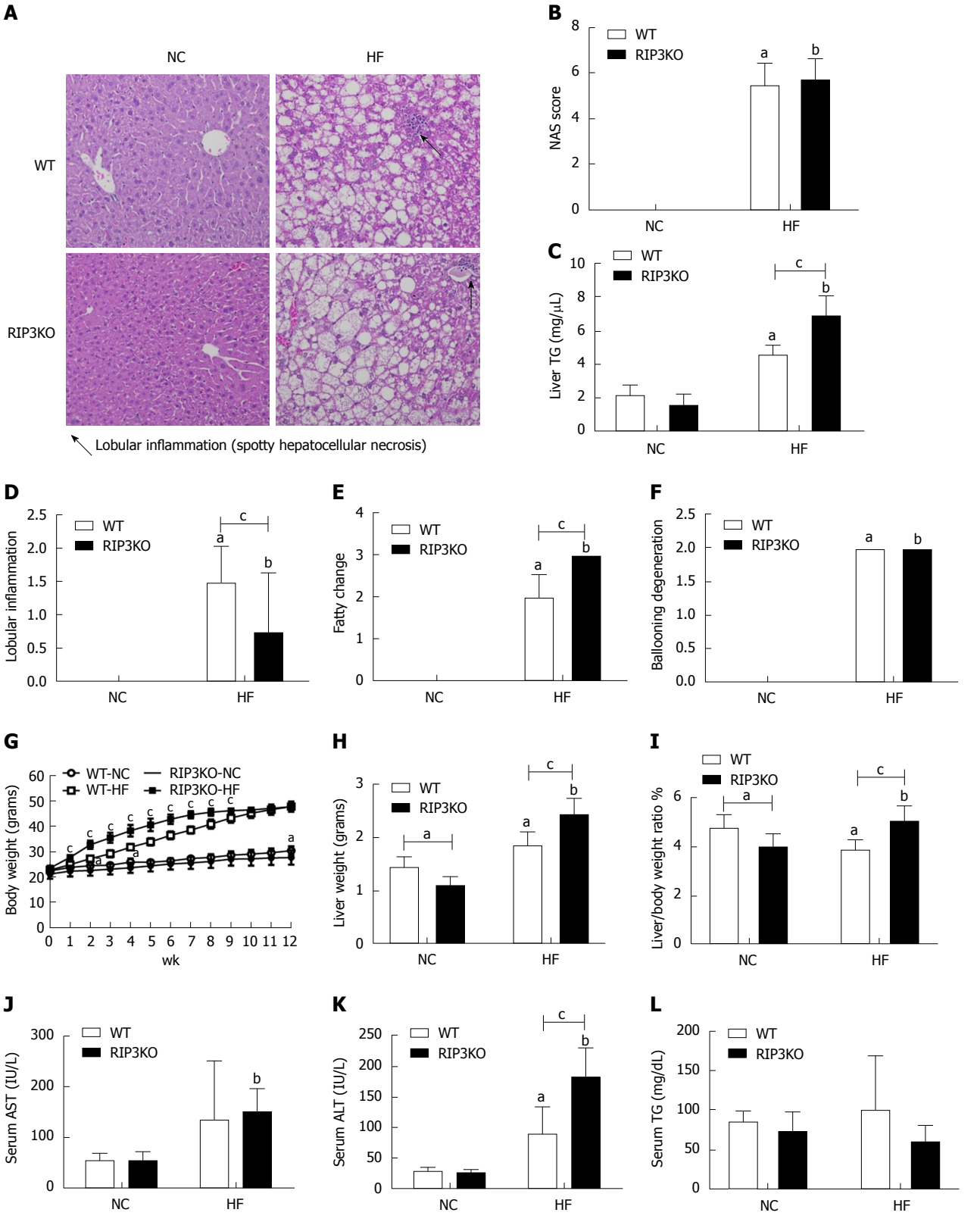

Figure 1 Receptor interacting protein kinase-3 deletion exacerbates HF diet induced steatosis. A: Following 12-wk HF diet, the liver tissue hematoxylin & eosin staining showed increased steatosis in RIP3KO-HF group compared to WT-HF group. B-F: Liver TG contents were significantly increased in the RIP3KO-HF group compared to the WT-HF group. RIP3KO-HF group had increased steatosis and decreased lobular inflammation. G-L: HF diet fed RIP3KO mice had increased liver weight and liver/body weight ratio compared to HF diet fed WT mice. The RIP3KO-HF group had increased serum AST and ALT but decreased serum TG compared to the WT-HF group. [a]*P* < 0.05 by Mann-Whitney *U* test, compared to NC diet fed WT group; [b]*P* < 0.05 by Mann-Whitney *U* test, compared to NC diet fed RIP3-KO group; [c]*P* < 0.05 by Mann-Whitney *U* test, compared to HF diet fed WT group. HF: High fat; NC: Normal chow; WT: Wild-type; KO: Knockout; RIP3: Receptor interacting protein kinase-3; AST: Aspartate aminotransferase; ALT: Alanine aminotransferase; TG: Triglycerides.

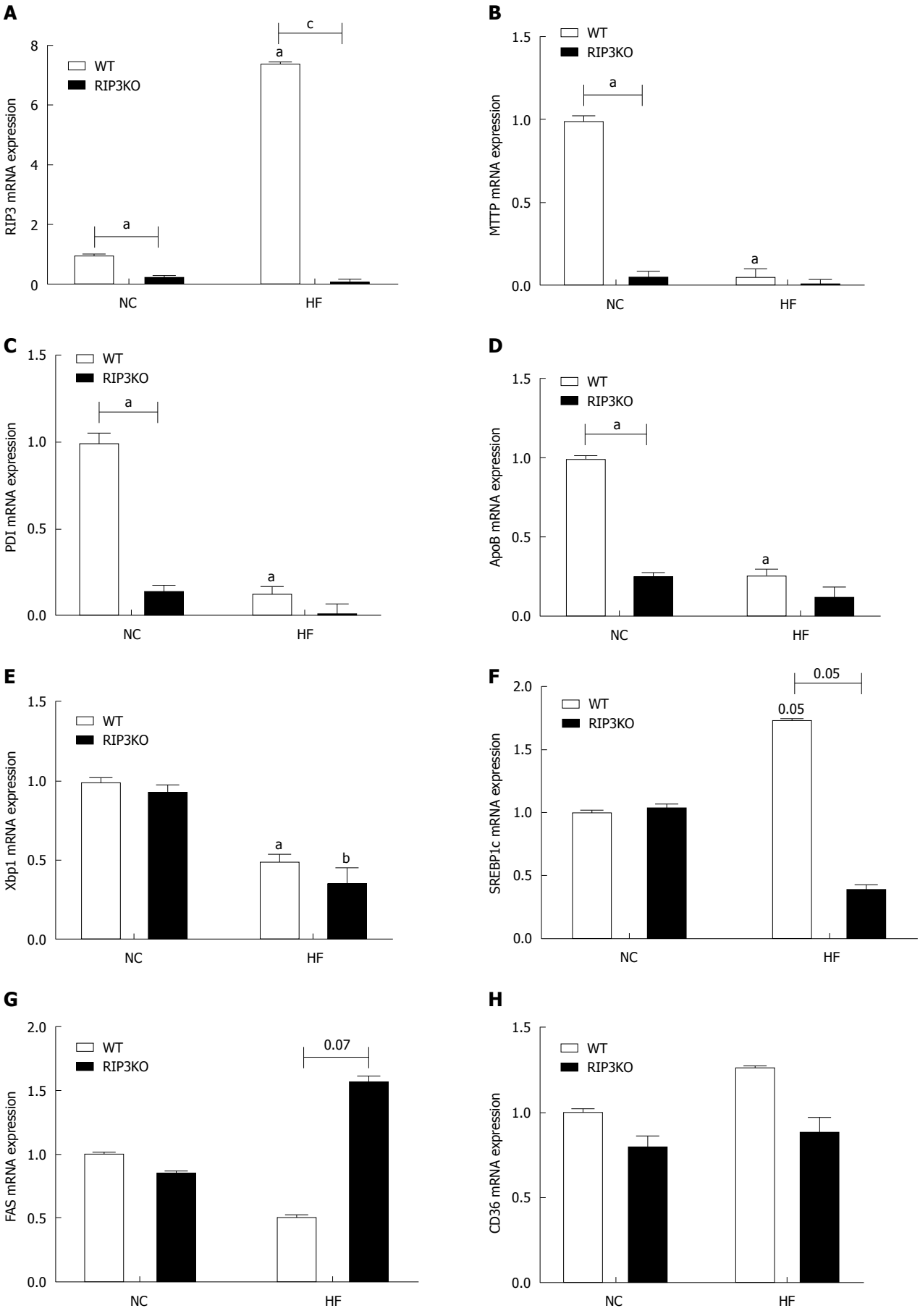
A
RIP3 mRNA expression
WT
RIP3KO
a
a
c
NC
HF
B
MTTP mRNA expression
WT
RIP3KO
a
a
NC
HF
C
PDI mRNA expression
WT
RIP3KO
a
a
NC
HF
D
ApoB mRNA expression
WT
RIP3KO
a
a
NC
HF
E
Xbp1 mRNA expression
WT
RIP3KO
a
b
NC
HF
F
SREBP1c mRNA expression
WT
RIP3KO
0.05
0.05
NC
HF
G
FAS mRNA expression
WT
RIP3KO
0.07
NC
HF
H
CD36 mRNA expression
WT
RIP3KO
NC
HF

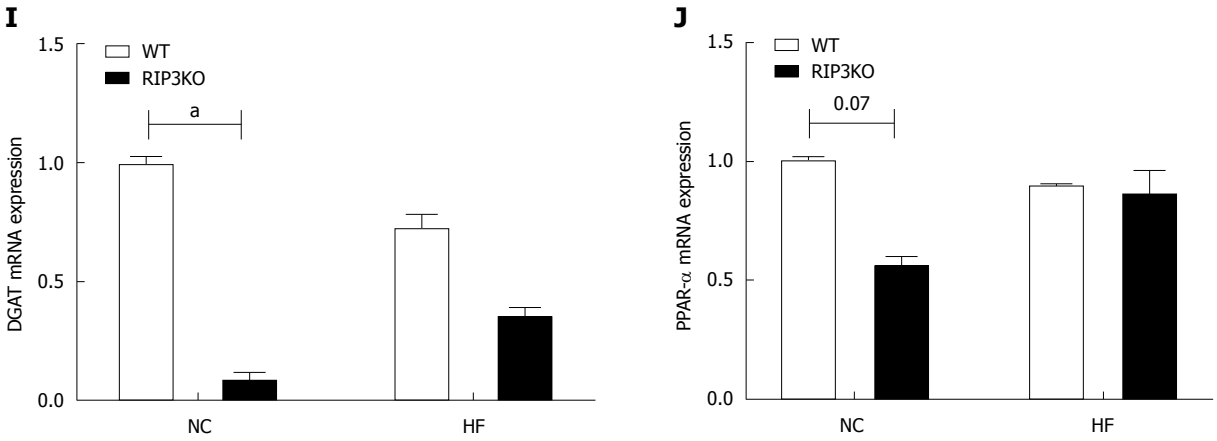

Figure 2 Effect of receptor interacting protein kinase-3 deletion on fat synthesis. A-J: Quantitative real-time PCR analysis showed an increased expression of RIP3 the WT-HF group after HF diet feeding. Interestingly, very-low-density lipoprotein secretion markers including apolipoprotein-B, microsomal triglyceride transfer protein, protein disulfide isomerase, and X-box binding protein-1 were decreased in the RIP3KO-HF group compared to the WT-HF group. The differences in SREBP1c, FAS, CD36, DGAT, and PPAR-α were not definite. [a]*P* < 0.05 by Mann-Whitney *U* test, compared to NC diet fed WT group; [b]*P* < 0.05 by Mann-Whitney *U* test, compared to NC diet fed RIP3-KO group; [c]*P* < 0.05 by Mann-Whitney *U* test, compared to HF diet fed WT group. HF: High fat; KO: Knockout; NC: Normal chow; WT: Wild-type; RIP3: Receptor interacting protein kinase-3; VLDL: Very-low-density lipoproteins; ApoB: Apolipoprotein-B; MTTP: Microsomal triglyceride transfer protein; PDI: Protein disulfide isomerase; XBP1: X-box binding protein-1; SREBP1c: Sterol regulatory element-binding protein-1c; FAS: Fatty acid synthase; CD36: Cluster of differentiation-36; DGAT: Diglyceride acyltransferase; PPAR-α: Peroxisome proliferator-activated receptor alpha.

SYBRGreen I Mastermix (Roche Diagnostics) in standard 10 μL reaction volumes as follows: 4 μL (100 ng) cDNA, 0.5 μL of 10 pmol/L sense primer, 0.5 μL of 10 pmol/L antisense primer, and 5 μL LightCycler 480 SYBRGreen I Mastermix (Roche Diagnostics). To guarantee the reliability of the obtained results, all samples were processed in triplicate and performed using a negative control. The values obtained were normalized to the control and expressed as fold changes.

Statistical analysis

The values are expressed as mean ± standard deviation. Statistical analysis was performed using SPSS for Windows version 21.0 (IBM Corp., Armonk, NY, United States). All experiments were performed three times. One-way analysis of variance and the Mann-Whitney *U* test were performed to compare the mean of different groups, and a *P*-value < 0.05 was considered significant.

RESULTS

Exacerbated intrahepatic fat amount but attenuated hepatic inflammation in HF diet fed RIP3KO mice

RIP3KO mice showed increased hepatic fat deposition on histological and hepatic tissue TG contents analysis compared to WT mice (4.58 nm/μL *vs* 6.92 nm/μL, *P* = 0.000) when fed with 60% HF but not with normal chow diet (Figure 1A and C). Body weight was significantly increased in HF diet fed RIP3KO mice compared to WT mice. Overall, NAS score was not significantly different between the both WT-HF and RIP3KO-HF groups; however, fatty change was significantly increased (2 *vs* 3, *P* = 0.000) and lobular inflammation was decreased (1.5 *vs* 0.75, *P* = 0.007) in HF fed RIP3KO mice (Figure 1B, D-F). Liver weight (1.87 g *vs* 2.43 g, *P* = 0.001) and liver to body weight ratio (5.09 *vs* 3.91, *P* = 0.000) were also increased in HF diet fed RIP3KO mice compared to WT mice (Figure 1H and I). Serum ALT was increased in HF diet fed RIP3KO mice (Figure 1K).

Effect of RIP3 ablation on hepatic fat regulation

RIP3 expression increased with the HF diet (Figure 2A), as previously observed[18]. The expression of other genes involved in lipid homeostasis, including those for sterol regulatory element-binding protein-1c, fatty acid synthase, cluster of differentiation-36, diglyceride acyltransferase, and peroxisome proliferator-activated receptor alpha, were not definite (Figure 2F-J). The genes involved in very-low-density lipoprotein (VLDL) secretion were analyzed to evaluate increased hepatic tissue TG contents. The mRNA analysis showed that RIP3KO mice had significantly decreased VLDL secretion markers, including microsomal triglyceride transfer protein (MTTP), protein disulfide isomerase (PDI), and apolipoprotein-B (ApoB). VLDL secretion markers were further suppressed in HF diet fed RIP3KO animals (Figure 2B-D).

Next, to confirm whether the effect of RIP3 deletion could also be observed *in vitro*, primary hepatocytes from WT and RIP3KO mice were isolated. Following treatment with OA, Nile red staining was increased in both WT and RIP3KO primary hepatocytes. However, OA treated RIP3KO primary hepatocytes had increased Nile red staining compared to WT primary hepatocytes (Figure 3A). Next, to confirm further, RIP3 was overexpressed in primary hepatocytes using an RIP3 overexpression system. If RIP3 ablation exacerbates hepatic lipid storage, then RIP3 overexpression should decrease lipid storage. As expected, RIP3 overexpressed

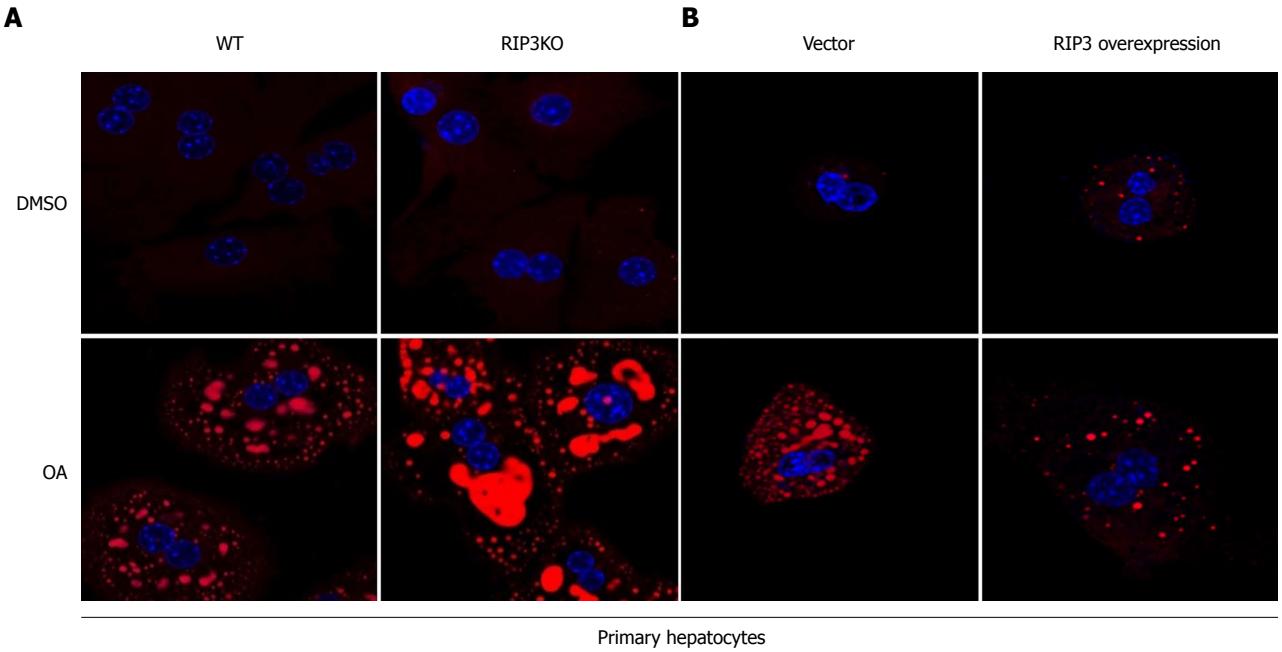
A
WT
RIP3KO
DMSO
OA
B
Vector
RIP3 overexpression
Primary hepatocytes

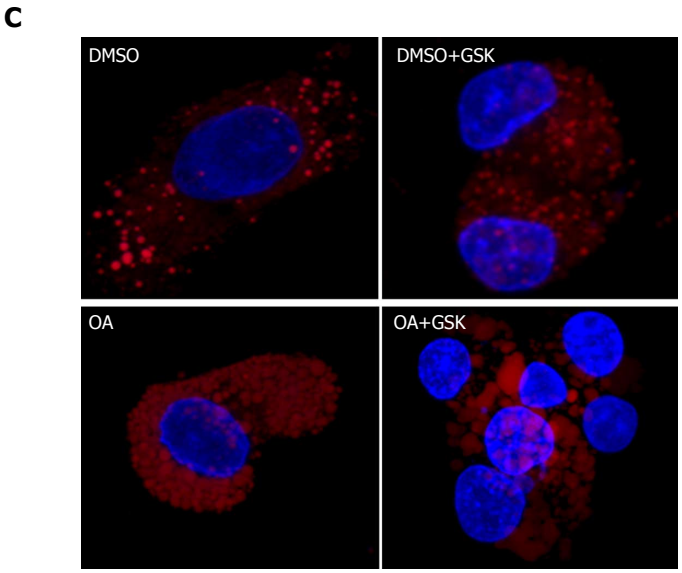
C
DMSO
DMSO+GSK
OA
OA+GSK

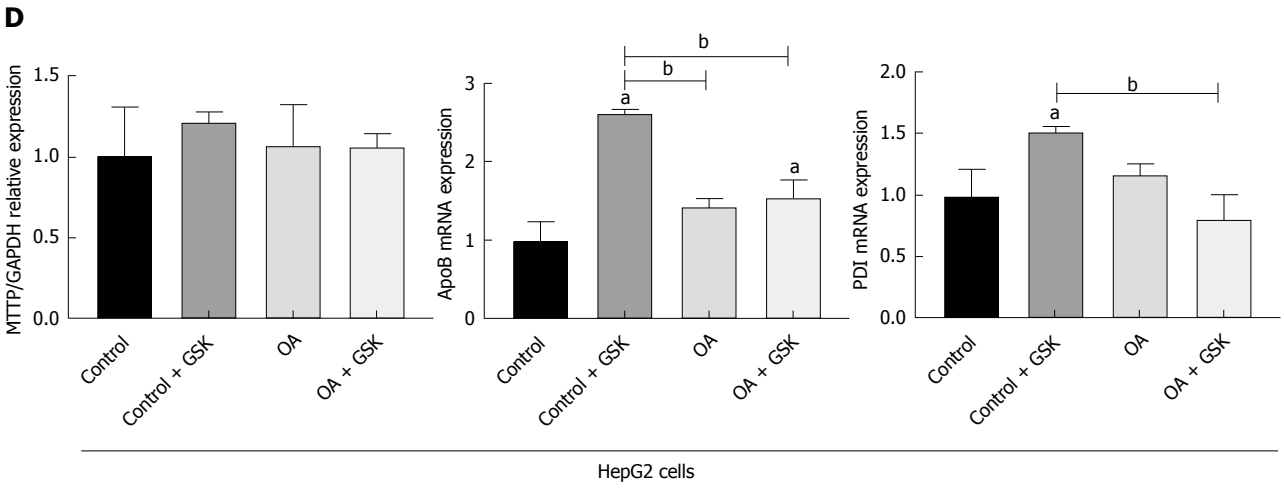
D
MTTP/GAPDH relative expression
1.5
1.0
0.5
0.0
Control
Control + GSK
OA
OA + GSK
ApoB mRNA expression
3
2
1
0
a
b
PDI mRNA expression
2.0
1.5
1.0
0.5
0.0
HepG2 cells

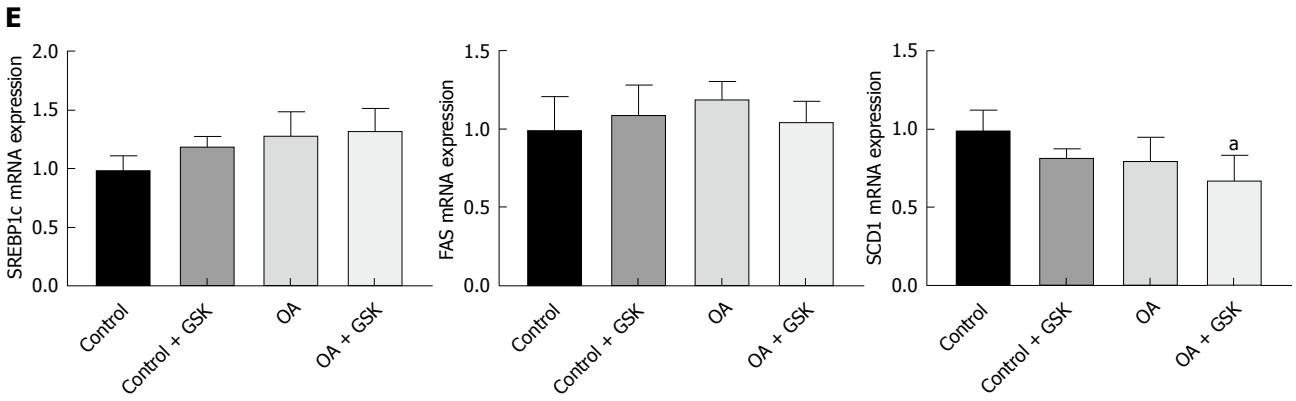

Figure 3 RIP3 deletion increases hepatic fat storage. A and B: The primary hepatocytes from WT and RIP3KO mice were treated with DMSO and OA. The RIP3KO primary hepatocytes had increased Nile red staining compared to WT primary hepatocytes. RIP3 overexpression decreased Nile red staining compared to the vector group treated with OA. C and D: HepG2 cells treated with GSK'843 did not show increase Nile red staining. The expression of MTTP, PDI, and ApoB was also not decreased in GSK'843 treated HepG2 cells. E: GSK'843 treatment did not increase the expression of SREBP1c, FAS, and SCD-1 in HepG2 cells. [a]*P* < 0.05 by ANOVA, Duncan post hoc analysis, compared to control; [b]*P* < 0.05 by ANOVA, Duncan post hoc analysis. WT: Wild-type; RIP3: Receptor interacting protein kinase-3; KO: Knockout; DMSO: Dimethyl sulfoxide; OA: Oleic acid; ApoB: Apolipoprotein-B; MTTP: Microsomal triglyceride transfer protein; PDI: Protein disulfide isomerase; XBP1: X-box binding protein-1; SREBP1c: Sterol regulatory element-binding protein-1c; FAS: Fatty acid synthase; SCD-1: Stearyl-CoA desaturase-1; ANOVA, Analysis of variance.

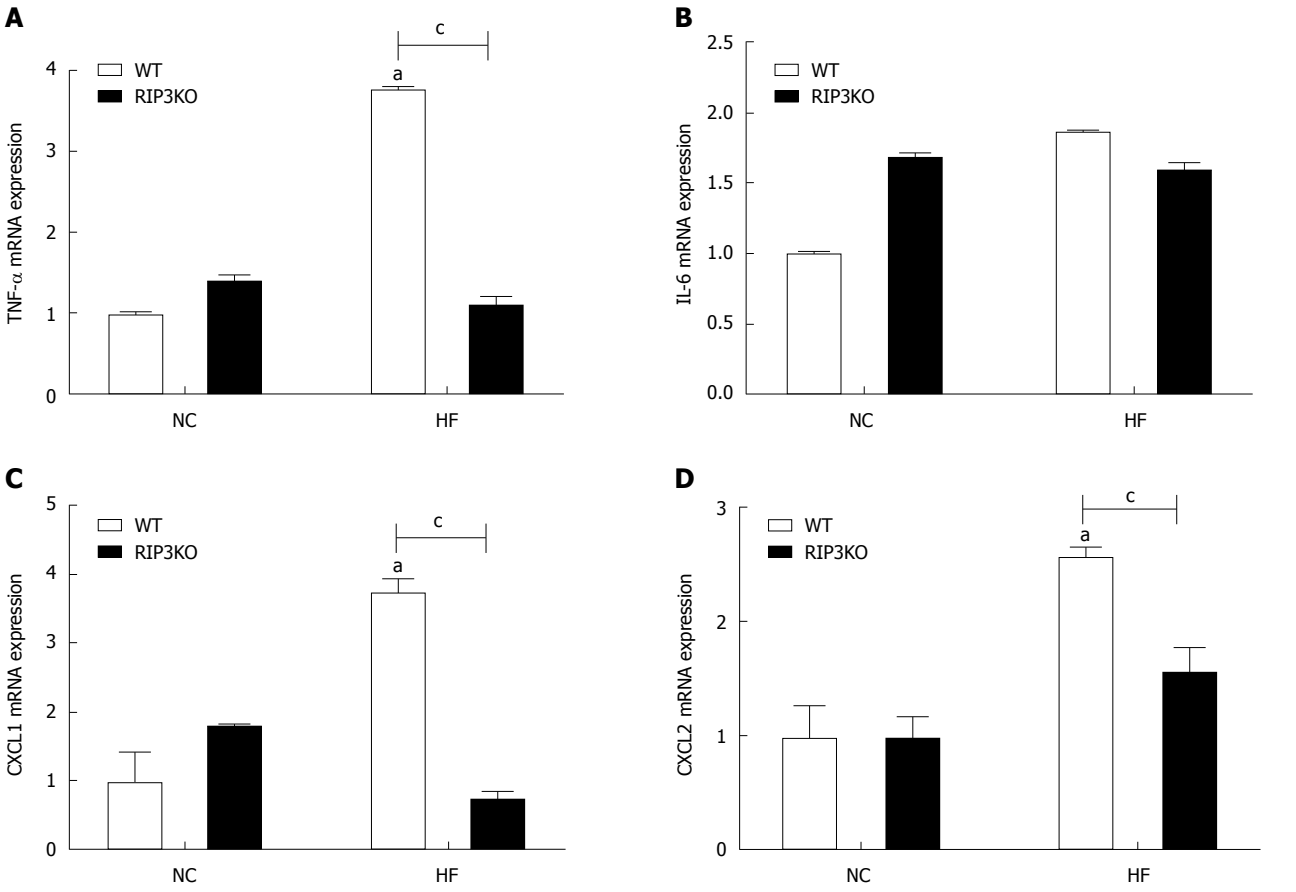

Figure 4 RIP3 reduces inflammation in liver tissue. Following HF diet feeding, RIP3KO mice had reduced expression of TNF-α, CXCL1, and CXCL2 compared to HF diet fed WT mice. [a]*P* < 0.05 by Mann-Whitney *U* test, compared to NC diet fed WT group; [c]*P* < 0.05 by Mann-Whitney *U* test, compared to HF diet fed WT group. HF: High fat; KO: Knockout; WT: Wild-type; NC: Normal chow; RIP3: Receptor interacting protein kinase-3; TNF-α: Tumor necrosis factor alpha; CXCL1: Chemokine (C-X-C motif) ligand-1; CXCL2: Chemokine (C-X-C motif) ligand-2.

primary hepatocytes had decreased Nile red staining compared to control (Figure 3B). Next, we evaluated whether RIP3 inhibition using GSK'843 would also yield similar results in HepG2 cells. However, GSK'843 treated HepG2 cells did not show an increase in Nile red staining, a decrease in MTTP, PDI, and ApoB expression (Figure 3C and D), and changes in sterol regulatory element-binding protein-1c, fatty acid synthase, and

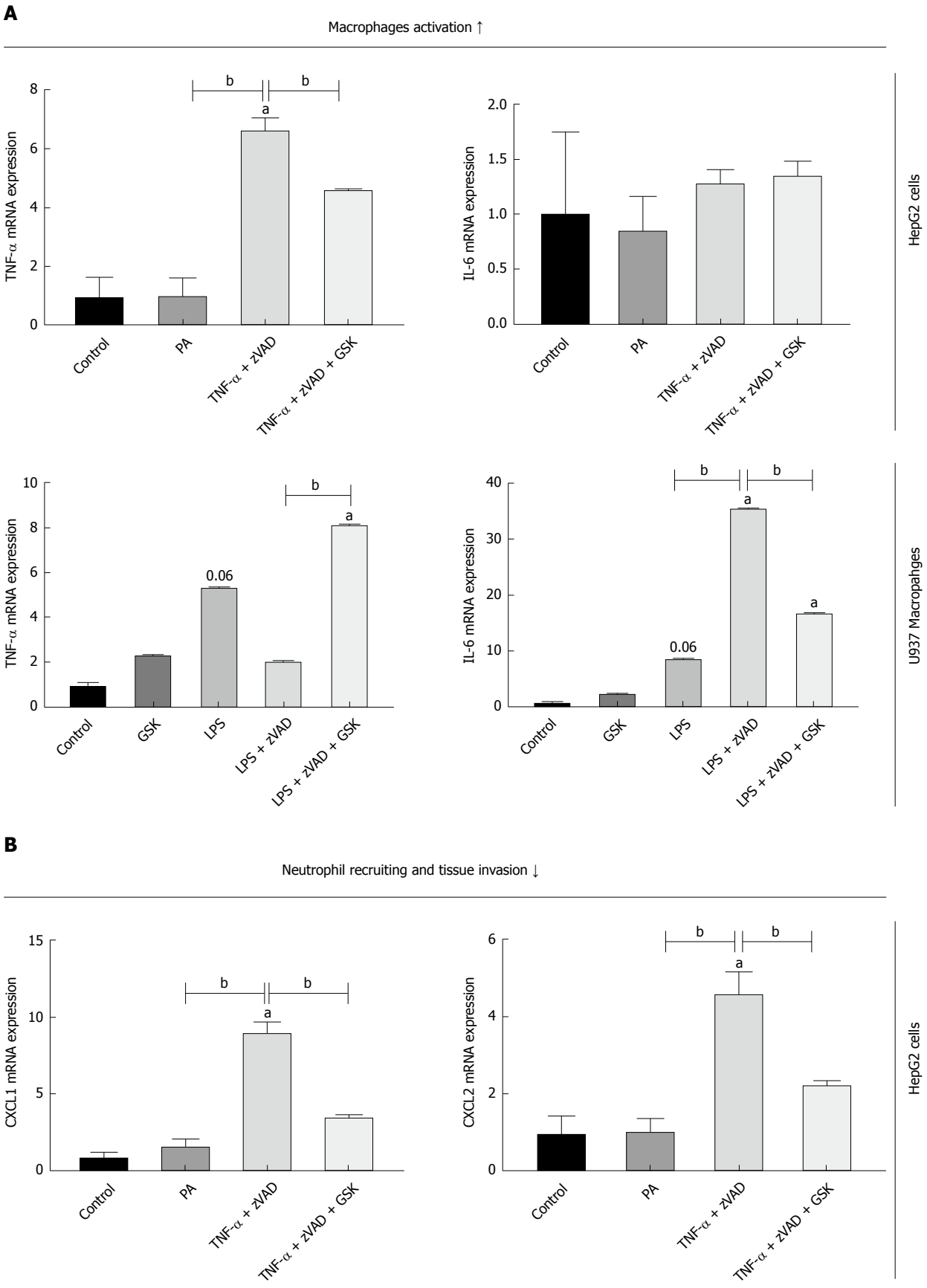
A
Macrophages activation ↑
TNF-α mRNA expression
IL-6 mRNA expression
Control
PA
TNF-α + zVAD
TNF-α + zVAD + GSK
HepG2 cells
GSK
LPS
LPS + zVAD
LPS + zVAD + GSK
U937 Macropahges
B
Neutrophil recruiting and tissue invasion ↓
CXCL1 mRNA expression
CXCL2 mRNA expression
HepG2 cells

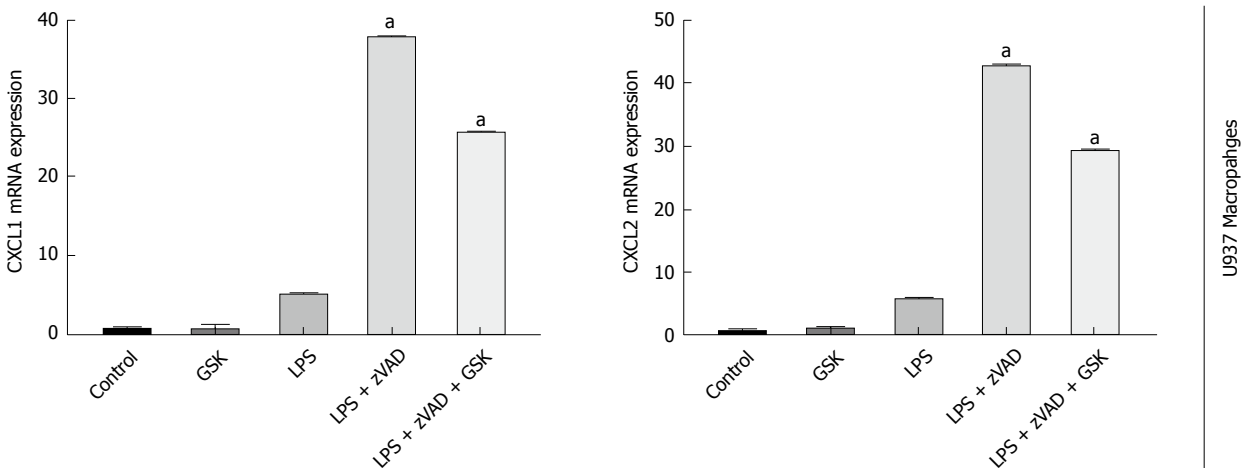

Figure 5 Effect of RIP3 on inflammatory markers. A and B: TNF-α/LPS + zVAD induced increase in TNF-α expression was exacerbated with GSK'843 treatment. TNF-α/LPS + zVAD induced increased expression of CXCL1 and CXCL2 was decreased with GSK'843 treatment. [a]*P* < 0.05 by ANOVA, Duncan post hoc analysis, compared to control; [b]*P* < 0.05 by ANOVA, Duncan post hoc analysis. TNF-α: Tumor necrosis factor alpha; LPS: Lipopolysaccharide; zVAD: N-Benzyloxycarbonyl-Val-Ala-Asp(O-Me) fluoromethyl ketone; CXCL1: Chemokine (C-X-C motif) ligand-1; CXCL2: Chemokine (C-X-C motif) ligand-2; ANOVA, Analysis of variance.

stearyl-CoA desaturase (SCD-1) expression (Figure 3E).

RIP3 partially regulated macrophage activation

HF diet fed RIP3KO mice had reduced expression of TNF-α, CXCL1, and CXCL2 compared to HF diet fed WT mice (Figure 4A-D). *In vitro* analysis suggested that necroptotic stimulation (LPS + zVAD) increased CXCL1/2 expression in monocytes. RIP3 inhibitor (GSK' 843) decreased the expression of CXCL1/2 as well as IL-6, but GSK'843 did not reduce TNF-α expression. The levels of neutrophil chemokines (CXCL1, and CXCL2) were decreased with GSK'843 (Figure 5A and B).

DISCUSSION

Our results suggest that RIP3 inhibition is associated with suppression of VLDL secretion markers and partial inhibition of macrophage activation *via* inhibiting CXCL1 and 2 expressions.

Previously, varying results of RIP3 inhibition in HF and MCD diet-induced animal NAFLD models were observed. In HF diet-induced NAFLD model[18], RIP3 deletion was associated with increased fatty change, hepatic tissue TG, body weight, and serum AST and ALT. Another study, however, reported that in the MCD diet-induced NAFLD model, RIP3 deletion did not affect lipidosis score in the early phase (2-wk) but did decrease it in the late phase (8 wk)[11]. The MCD diet-induced NAFLD studies did not extensively evaluate for hepatic steatosis[11,12]. None of the previous studies examined the precise mechanism of hepatic fat accumulation and the interaction with hepatocytes pathways of lipid *de novo* synthesis, transportation, and metabolism. Our results also showed that VLDL secretion markers, including ApoB, MTTP, and PDI, were suppressed with RIP3 deletion (Figure 2). The primary hepatocytes isolated from WT and RIP3KO mice were treated with DMSO and OA. Similar to increased hepatic TG contents in RIP3KO mice, OA treated RIP3KO primary hepatocytes had increased Nile red staining compared to OA treated WT primary hepatocytes. Correspondingly, primary hepatocytes overexpressing RIP3 also showed decreased Nile red staining compared to control (Figure 3). However, we did not observe a decrease in the expression of MTTP, PDI, and ApoB following treatment with GSK'843 in HepG2 cells.

Similar to previous findings[13], our results showed that the overall NAS score was the same between HF diet fed WT and RIP3KO mice; however, lobular inflammation was decreased in our study. Moreover, in contrast to the MCD diet-induced NAFLD model, RIP3 deletion associated reductions in serum AST and ALT were not observed in our study. On the contrary, in HF diet-induced NAFLD model, RIP3 induction was thought to protect hepatocytes against further steatosis and, thus, the RIP3 deletion might have led to more deleterious effects[18]. Moreover, RIP3 deletion was also associated with exacerbated inflammation in the HF diet-induced NAFLD[18]. Interestingly, RIP3 deletion reduced ethanol induced steatosis[22]. In our study, following HF diet feeding, CXCL1/2 expression increased in liver tissue. The expressions of CXCL1/2 were reduced in RIP3KO mice compared to corresponding controls. *In vitro*, TNFα/LPS + zVAD induced CXCL1/2 expressions. GSK'843 treatment reduced CXCL1 and CXCL2 expression in U937 macrophages and HepG2 cells, but TNF-α expression was not reduced (Figures 5 and 6).

Our study has the following limitations. First, we did not evaluate the long-term effects of RIP3 deletion on the exacerbated response in HF diet-induced NAFLD model. Moreover, we did not evaluate the previously highlighted contribution of increased hepatic and adipose tissue apoptosis associated with RIP3 deletion

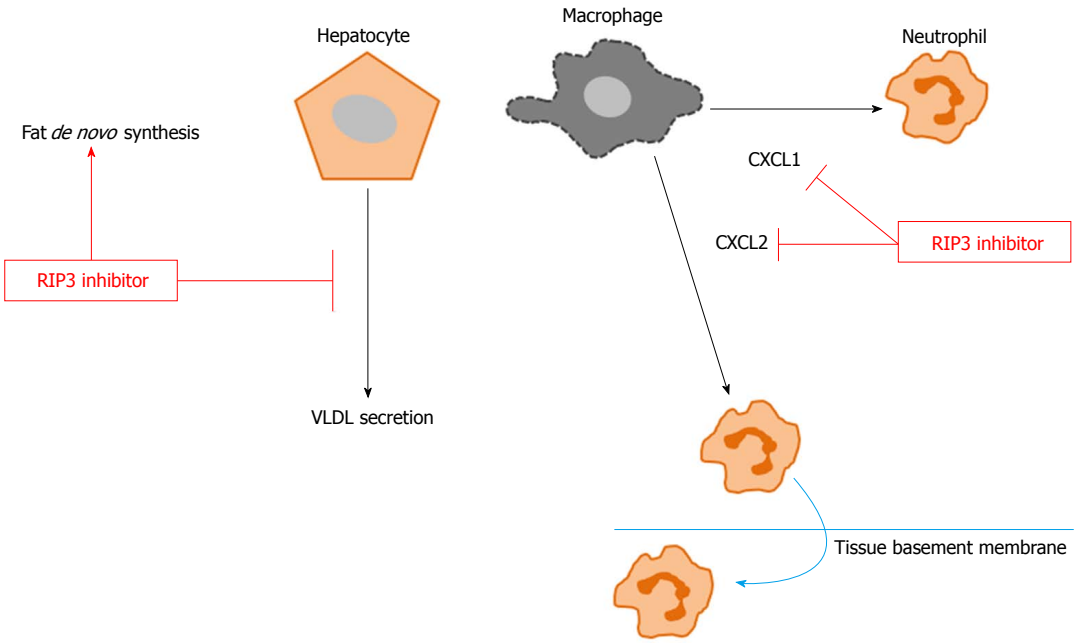

Figure 6 Conceptual diagram. GSK'843 treatment decreases neutrophil recruitment markers, including CXCL1 and CXCL2, thereby reducing neutrophil recruitment to the tissue. However, RIP3 inhibition increases *de novo* fat synthesis while decreasing VLDL secretion. RIP3: Receptor interacting protein kinase-3; CXCL1: Chemokine (C-X-C motif) ligand-1; CXCL2: Chemokine (C-X-C motif) ligand-2; VLDL: Very-low-density lipoproteins.

in NAFLD. RIP3 ablation in adipose tissue leads to the metabolic phenotype in RIP3KO mice. Moreover, RIP3 has a role in maintaining white adipose tissue homeostasis and systemic RIP3 ablation leads to insulin resistance and glucose intolerance. RIP3 overexpression is thought to balance caspase-8 mediated increase in apoptosis. Following RIP3 deletion, a switch towards increased apoptosis in both liver and adipose tissues was observed, and increased adipocytes apoptosis was thought to mediate the systemic effects[13]. Therefore, to elaborate the detailed mechanism of additional *in vivo* signaling, a further in depth analysis is needed. Second, examination of hepatocyte specific RIP3 knockout and RIP3 kinase dead mice would be useful to understand HF diet-induced NAFLD. The pathogenic context, initiating stimulus, and compartment specific RIP3 regulation[12,13] might reveal why such diverse results of RIP3 deletion are observed in the NAFLD models. Other studies also reported that the expression of regulated necrosis molecules could be different according to the trigger, disease pathogenesis, organs involved, and species[23]. Moreover, studies have also suggested that different cell types could be responding differentially to necroptosis stimuli[13].

In conclusion, our results show that RIP3 deletion aggravates hepatic steatosis in the HF diet-induced NAFLD model. RIP3 deletion was also associated with suppression of VLDL secretion from hepatocytes. Moreover, targeting RIP3 could have deleterious systemic consequences. Future research should consider the diverse and unwanted systemic consequences of RIP3 deletion in NAFLD. The role of RIP3 could be a double-edged sword in NAFLD. Although RIP3 has a crucial role in necroptosis, RIP3 showed diverse effects in metabolic disease. Therefore, careful attention and more extensive studies are needed to further elaborate the interactions between RIP3 and NAFLD associated signaling pathways.

ARTICLE HIGHLIGHTS

Research background

The receptor interacting protein kinase-3 (RIP3) inhibition in various non-alcoholic fatty liver disease (NAFLD) models has shown varied results. The underlying mechanism associated with these diverse outcomes is still not clear. The evaluation of necroptosis signaling molecules in NAFLD might provide a useful therapeutic target.

Research motivation

Previous studies report that in high fat (HF)-induced NAFLD, RIP3 deletion exacerbated fatty change, inflammation, fibrosis, and apoptosis. However, in the methionine choline deficient diet-induced NAFLD model, these changes were not observed. The reason for the varied results associated with RIP3 deletion in different NAFLD models is unknown.

Research objective

To validate the effects of RIP3 deletion in NAFLD and to clarify the mechanism of action.

Research methods

Wild-type and RIP3 knockout mice were fed HF and normal chow diets for 12 wk. The body weight was assessed weekly. After 12 wk, the liver and serum samples were analyzed for changes. Hematoxylin & eosin staining, NAFLD Activity Score evaluation, and triglyceride quantification were performed. The changes in very-low-density lipoproteins (VLDL) secretion and inflammation markers were recorded. Primary hepatocytes were evaluated for lipid contents. HepG2 cells and U937 cells were evaluated for changes in inflammatory

markers.

Research results

Our results show that RIP3 deletion is associated with exacerbated hepatic lipid contents, suppressed VLDL secretion markers, and partially suppressed inflammation.

Research conclusion

In HF diet-induced NAFLD, RIP3 deletion is associated with increased hepatic steatosis and partially suppressed inflammation

Research perspective

Necroptosis signaling molecules, especially mixed lineage kinase domain-like proteins, should be further explored for its therapeutic potential in NAFLD.

REFERENCES

1 **Fingas CD,** Best J, Sowa J-P, Canbay A. Epidemiology of nonalcoholic steatohepatitis and hepatocellular carcinoma. *Clinical Liver Disease* 2016; **8:** 119-122 [DOI: 10.1002/cld.585]

2 **Trovato FM**, Martines GF, Catalano D, Musumeci G, Pirri C, Trovato GM. Echocardiography and NAFLD (non-alcoholic fatty liver disease). *Int J Cardiol* 2016; **221**: 275-279 [PMID: 27404689 DOI: 10.1016/j.ijcard.2016.06.180]

3 **Trovato FM**, Martines GF, Brischetto D, Catalano D, Musumeci G, Trovato GM. Fatty liver disease and lifestyle in youngsters: diet, food intake frequency, exercise, sleep shortage and fashion. *Liver Int* 2016; **36**: 427-433 [PMID: 26346413 DOI: 10.1111/liv.12957]

4 **Oh H**, Jun DW, Saeed WK, Nguyen MH. Non-alcoholic fatty liver diseases: update on the challenge of diagnosis and treatment. *Clin Mol Hepatol* 2016; **22**: 327-335 [PMID: 27729634 DOI: 10.3350/cmh.2016.0049]

5 **Bessone F**, Razori MV, Roma MG. Molecular pathways of nonalcoholic fatty liver disease development and progression. *Cell Mol Life Sci* 2018 Epub ahead of print [PMID: 30343320 DOI: 10.1007/s00018-018-2947-0]

6 **Ipsen DH**, Lykkesfeldt J, Tveden-Nyborg P. Molecular mechanisms of hepatic lipid accumulation in non-alcoholic fatty liver disease. *Cell Mol Life Sci* 2018; **75**: 3313-3327 [PMID: 29936596 DOI: 10.1007/s00018-018-2860-6]

7 **Atay K**, Canbakan B, Koroglu E, Hatemi I, Canbakan M, Kepil N, Tuncer M, Senturk H. Apoptosis and Disease Severity is Associated with Insulin Resistance in Non-alcoholic Fatty Liver Disease. *Acta Gastroenterol Belg* 2017; **80**: 271-277 [PMID: 29560693]

8 **Farrell GC**, Haczeyni F, Chitturi S. Pathogenesis of NASH: How Metabolic Complications of Overnutrition Favour Lipotoxicity and Pro-Inflammatory Fatty Liver Disease. *Adv Exp Med Biol* 2018; **1061**: 19-44 [PMID: 29956204 DOI: 10.1007/978-981-10-8684-7_3]

9 **Galluzzi L**, Bravo-San Pedro JM, Vitale I, Aaronson SA, Abrams JM, Adam D, Alnemri ES, Altucci L, Andrews D, Annicchiarico-Petruzzelli M, Baehrecke EH, Bazan NG, Bertrand MJ, Bianchi K, Blagosklonny MV, Blomgren K, Borner C, Bredesen DE, Brenner C, Campanella M, Candi E, Cecconi F, Chan FK, Chandel NS, Cheng EH, Chipuk JE, Cidlowski JA, Ciechanover A, Dawson TM, Dawson VL, De Laurenzi V, De Maria R, Debatin KM, Di Daniele N, Dixit VM, Dynlacht BD, El-Deiry WS, Fimia GM, Flavell RA, Fulda S, Garrido C, Gougeon ML, Green DR, Gronemeyer H, Hajnoczky G, Hardwick JM, Hengartner MO, Ichijo H, Joseph B, Jost PJ, Kaufmann T, Kepp O, Klionsky DJ, Knight RA, Kumar S, Lemasters JJ, Levine B, Linkermann A, Lipton SA, Lockshin RA, López-Otín C, Lugli E, Madeo F, Malorni W, Marine JC, Martin SJ, Martinou JC, Medema JP, Meier P, Melino S, Mizushima N, Moll U, Muñoz-Pinedo C, Nuñez G, Oberst A, Panaretakis T, Penninger JM, Peter ME, Piacentini M, Pinton P, Prehn JH, Puthalakath H, Rabinovich GA, Ravichandran KS, Rizzuto R, Rodrigues CM, Rubinsztein DC, Rudel T, Shi Y, Simon HU, Stockwell BR, Szabadkai G, Tait SW, Tang HL, Tavernarakis N, Tsujimoto Y, Vanden Berghe T, Vandenabeele P, Villunger A, Wagner EF, Walczak H, White E, Wood WG, Yuan J, Zakeri Z, Zhivotovsky B, Melino G, Kroemer G. Essential versus accessory aspects of cell death: recommendations of the NCCD 2015. *Cell Death Differ* 2015; **22**: 58-73 [PMID: 25236395 DOI: 10.1038/cdd.2014.137]

10 **Saeed WK**, Jun DW. Necroptosis: an emerging type of cell death in liver diseases. *World J Gastroenterol* 2014; **20**: 12526-12532 [PMID: 25253954 DOI: 10.3748/wjg.v20.i35.12526]

11 **Afonso MB**, Rodrigues PM, Carvalho T, Caridade M, Borralho P, Cortez-Pinto H, Castro RE, Rodrigues CM. Necroptosis is a key pathogenic event in human and experimental murine models of non-alcoholic steatohepatitis. *Clin Sci* (Lond) 2015; **129**: 721-739 [PMID: 26201023 DOI: 10.1042/CS20140732]

12 **Gautheron J**, Vucur M, Reisinger F, Cardenas DV, Roderburg C, Koppe C, Kreggenwinkel K, Schneider AT, Bartneck M, Neumann UP, Canbay A, Reeves HL, Luedde M, Tacke F, Trautwein C, Heikenwalder M, Luedde T. A positive feedback loop between RIP3 and JNK controls non-alcoholic steatohepatitis. *EMBO Mol Med* 2014; **6**: 1062-1074 [PMID: 24963148 DOI: 10.15252/emmm.201403856]

13 **Gautheron J**, Vucur M, Schneider AT, Severi I, Roderburg C, Roy S, Bartneck M, Schrammen P, Diaz MB, Ehling J, Gremse F, Heymann F, Koppe C, Lammers T, Kiessling F, Van Best N, Pabst O, Courtois G, Linkermann A, Krautwald S, Neumann UP, Tacke F, Trautwein C, Green DR, Longerich T, Frey N, Luedde M, Bluher M, Herzig S, Heikenwalder M, Luedde T. The necroptosis-inducing kinase RIPK3 dampens adipose tissue inflammation and glucose intolerance. *Nat Commun* 2016; **7**: 11869 [PMID: 27323669 DOI: 10.1038/ncomms11869]

14 **Afonso MB**, Rodrigues PM, Simão AL, Ofengeim D, Carvalho T, Amaral JD, Gaspar MM, Cortez-Pinto H, Castro RE, Yuan J, Rodrigues CM. Activation of necroptosis in human and experimental cholestasis. *Cell Death Dis* 2016; **7**: e2390 [PMID: 27685634 DOI: 10.1038/cddis.2016.280]

15 **Dara L**, Johnson H, Suda J, Win S, Gaarde W, Han D, Kaplowitz N. Receptor interacting protein kinase 1 mediates murine acetaminophen toxicity independent of the necrosome and not through necroptosis. *Hepatology* 2015; **62**: 1847-1857 [PMID: 26077809 DOI: 10.1002/hep.27939]

16 **Deutsch M**, Graffeo CS, Rokosh R, Pansari M, Ochi A, Levie EM, Van Heerden E, Tippens DM, Greco S, Barilla R, Tomkötter L, Zambirinis CP, Avanzi N, Gulati R, Pachter HL, Torres-Hernandez A, Eisenthal A, Daley D, Miller G. Divergent effects of RIP1 or RIP3 blockade in murine models of acute liver injury. *Cell Death Dis* 2015; **6**: e1759 [PMID: 25950489 DOI: 10.1038/cddis.2015.126]

17 **Saeed WK**, Jun DW, Jang K, Chae YJ, Lee JS, Kang HT. Does necroptosis have a crucial role in hepatic ischemia-reperfusion injury? *PLoS One* 2017; **12**: e0184752 [PMID: 28957350 DOI: 10.1371/journal.pone.0184752]

18 **Roychowdhury S**, McCullough RL, Sanz-Garcia C, Saikia P, Alkhouri N, Matloob A, Pollard KA, McMullen MR, Croniger CM, Nagy LE. Receptor interacting protein 3 protects mice from high-fat diet-induced liver injury. *Hepatology* 2016; **64**: 1518-1533 [PMID: 27301788 DOI: 10.1002/hep.28676]

19 **Newton K**, Sun X, Dixit VM. Kinase RIP3 is dispensable for normal NF-kappa Bs, signaling by the B-cell and T-cell receptors, tumor necrosis factor receptor 1, and Toll-like receptors 2 and 4. *Mol Cell Biol* 2004; **24**: 1464-1469 [PMID: 14749364]

20 **Kleiner DE**, Brunt EM, Van Natta M, Behling C, Contos MJ, Cummings OW, Ferrell LD, Liu YC, Torbenson MS, Unalp-Arida A, Yeh M, McCullough AJ, Sanyal AJ; Nonalcoholic Steatohepatitis Clinical Research Network. Design and validation of a histological scoring system for nonalcoholic fatty liver disease. *Hepatology* 2005; **41**: 1313-1321 [PMID: 15915461 DOI: 10.1002/hep.20701]

21 **Riccalton-Banks L**, Bhandari R, Fry J, Shakesheff KM. A simple method for the simultaneous isolation of stellate cells and

hepatocytes from rat liver tissue. *Mol Cell Biochem* 2003; **248**: 97-102 [PMID: 12870660]

22 **Roychowdhury S**, McMullen MR, Pisano SG, Liu X, Nagy LE. Absence of receptor interacting protein kinase 3 prevents ethanol-induced liver injury. *Hepatology* 2013; **57**: 1773-1783 [PMID: 23319235 DOI: 10.1002/hep.26200]

23 **Honarpisheh M**, Desai J, Marschner JA, Weidenbusch M, Lech M, Vielhauer V, Anders HJ, Mulay SR. Regulated necrosis-related molecule mRNA expression in humans and mice and in murine acute tissue injury and systemic autoimmunity leading to progressive organ damage, and progressive fibrosis. *Biosci Rep* 2016; **36**: [PMID: 27811014 DOI: 10.1042/bsr20160336]

P- Reviewer: Kanda T, Musumeci G **S- Editor**: Ma RY
L- Editor: Filipodia **E- Editor**: Huang Y

Published by **Baishideng Publishing Group Inc**
7901 Stoneridge Drive, Suite 501, Pleasanton, CA 94588, USA
Telephone: +1-925-223-8242
Fax: +1-925-223-8243
E-mail: bpgoffice@wjgnet.com
Help Desk: https://www.f6publishing.com/helpdesk
https://www.wjgnet.com

ISSN 1007-9327